



Development and Comparison of Surface-Enhanced Raman Scattering Gold Substrates for In Situ Characterization of 'Model' Analytes in Organic and Aqueous Media

Elie Akanny¹ · Anne Bonhommé¹ · Laurence Bois² · Sylvain Minot¹ · Sandrine Bourgeois^{3,4} · Claire Bordes³ · François Bessueille¹

Received: 5 December 2018 / Accepted: 15 February 2019 / Published online: 21 February 2019
© The Tunisian Chemical Society and Springer Nature Switzerland AG 2019

Abstract

Surface-Enhanced Raman Spectroscopy (SERS) is a technique that provides high enhancement of Raman scattering from molecules adsorbed on a rough noble metal surface. The aim of this study was the development of convenient and reproducible in situ SERS methods suitable for the detection and the quantification of analytes in organic or aqueous media. For this purpose, we used a signal acquisition technique which simply consisted of recording the SERS signal in the bulk solution by using a Raman immersion probe close to the surface of the immersed solid SERS substrate. This method should be useful for on-line process analysis and more robust than conventional acquisition techniques that are generally based on a drying step which may induce heterogeneous analyte repartition onto the substrate surface, thus often requiring the use of SERS mapping technique to improve the signal reproducibility. In this study, two types of gold SERS substrates (metal nanostructures on a solid substrate and metal nanoparticles in suspension) were investigated and compared for the in situ characterization of two 'model' analytes, Rhodamine 6G (R6G) and 1,2-bis(4-pyridyl)ethylene (BPE), in aqueous and organic media. The solid substrate developed by sputtering deposition of a nanometric gold film onto a glass slide provided reproducible and stable SERS signals of BPE in organic media at concentration down to 10^{-12} M. But it appeared unusable in aqueous solutions due to the removal of the gold deposit. Despite an improvement of the deposit adhesion onto the substrate by using tetraethoxysilane/(3-mercaptopropyl) trimethoxysilane sol or the use of an electroless deposition technique, the developed solid substrates did not allow to reach satisfying R6G SERS signal in aqueous solutions. Therefore, both star-like and spherical gold nanoparticles were finally developed and used as SERS substrates. After aggregation, colloids induced the best enhancement of R6G Raman signal with a possible quantification at concentrations down to $5 \cdot 10^{-9}$ M.

Keywords Surface enhanced Raman scattering (SERS) · Gold SERS substrates · In-situ characterization · Reproducibility · SERS quantification

✉ Elie Akanny
elie.kouame-akanny@univ-lyon1.fr

¹ Institut des Sciences Analytiques, UMR 5280, CNRS, ENS Lyon – 5, Université Lyon 1, Université de Lyon, Rue de la Doua, 69100 Villeurbanne, France

² Laboratoire des Multimatiériaux et Interfaces, UMR CNRS 5615, Bat. Berthollet, Université Claude Bernard- Lyon 1, 43 Bd 11 Novembre 1918, 69622 Villeurbanne, France

³ Laboratoire d'Automatique et de Génie des Procédés, UMR CNRS 5007, Université Lyon 1, Université de Lyon, 69622 Villeurbanne, France

⁴ ISPB-School of Pharmacy, Université Lyon 1, Université de Lyon, 69008 Lyon, France

1 Introduction

Raman spectroscopy is a well described technique for obtaining both quantitative and qualitative information on analytes. However due to the weakness of the conventional Raman signal, this technique requires highly concentrated samples. Observed for the first time in 1973 [1], Surface-Enhanced Raman Spectroscopy (SERS) is a technique that provides high enhancement of the Raman scattering from molecules adsorbed on a rough metal surface, such as silver, gold and copper [2]. Two phenomena are currently well-accepted to explain the SERS effect: an electromagnetic effect (EE) and a chemical effect (CE). EE arises from resonance between monochromatic electromagnetic waves and

the surface plasmon of the metallic nanostructure leading to the generation of intense electromagnetic fields at ‘hot-spot’ zones [3]. CE is induced by a charge-transfer between the chemisorbed analyte and the substrate which can change the polarizability of the molecule, resulting in a change of the Raman scattering cross-section of the molecule [4]. Moreover, CE is generally weaker than EE: being responsible for up to about 10^2 increase of Raman scattering instead of 10^6 – 10^7 for EE [2].

The predominant EE is strongly related to the structure of the SERS substrates. Therefore, one of the key challenges is the preparation of these substrates since a small variation in the final structure can cause significant changes in both the performance and reproducibility of the signal. The use of nanoparticles in suspension is the simplest method to obtain an effective SERS structure; but it is often poorly reproducible due to the need of nanoparticles aggregation for Raman signal enhancement. In the objective of increasing reproducibility, the development of nanostructures on solid substrates is shown to be an interesting pathway for producing SERS active structures. However, the increased reproducibility is often related to a loss of the exaltation efficiency of the Raman signal compared to nanoparticles in suspension [5]. The development of SERS substrates thus requires a compromise between reproducibility and exaltation efficiency.

Strategies to obtain SERS active nanostructures on solid substrates can mainly be classified as top-down and bottom-up approaches. In the case of top-down approaches, the oldest used electrochemical roughening technique [6–8] leading to the poor control of the shape and size of the nanostructure [9] and thus to low signal reproducibility, substrates based on lithographic techniques (e.g. E-beam lithography [10], nanosphere lithography [11, 12], soft-lithography [13]) or sputtering deposition have earned interest [14–16]. Indeed, these techniques allow to provide a large-scale uniformity of the structures with various shapes ensuring high SERS signal reproducibility. Bottom-up approaches concern the immobilisation of gold nanoparticles on a solid support. The most straightforward methods consist of the use of bifunctional linker molecules making the link between the nanoparticles and the solid support [9, 17] or the use of electroless deposition processes [18]. The immobilisation of nanoparticles on a solid support using sol–gel materials can also be found offering unique environment for stabilizing metal colloids [19, 20]. Among the many available techniques, it should be noted that the combination of bottom-up and top-down approaches can also be found and may appear interesting when taking the advantages of each technique [21, 22].

The signal acquisition method also has an importance in signal enhancement efficiency and reproducibility. In case of solid SERS substrates, SERS signal is generally measured after the drying of a drop of analyte deposited on the

substrate or after the drying of the substrate dipped in an analyte solution. But these drying processes often lead to heterogeneous analyte repartition on the substrate surface requiring the use of SERS mapping in order to obtain reproducible SERS signals [23–27].

In this context, the aim of this study was to develop SERS methods employing gold substrates suitable for the in situ detection and quantification of two ‘model’ analytes, Rhodamine 6G (R6G) and 1,2-bis(4-pyridyl)ethylene (BPE)), in aqueous or organic media. We have chosen to base these methods on an unusual signal acquisition technique which simply consisted of recording the SERS signal in the bulk solution by the means of a Raman immersion probe close to the surface of the immersed solid substrate. Such in situ characterization method, suitable in aqueous or organic media, should have many advantages: (i) to be more robust than conventional acquisition techniques, avoiding the critical drying stage (ii) the possibility of on-line process analysis, and (iii) in the case of sensitive analytes, the prevention from thermal degradation phenomena that could occur in the dry state. To our knowledge, this acquisition strategy has not been deeply explored previously, this is what has motivated this work. In this study, we investigated and compared different types of SERS substrates: gold nanostructures on a solid substrate (obtained by using sputtering deposition, soft lithography processes or electroless deposition) and gold nanoparticles in suspension synthesized by hydroxylamine reduction in basic conditions [28] or Frens method [29].

2 Materials and Methods

2.1 Materials

Hydrogen tetrachloroaurate(III) hydrate (HAuCl_4), sodium chloride (NaCl), silver nitrate (AgNO_3) were purchased from Alfa Aesar, Hydroxylamine solution 50% (wt), trisodium citrate, rhodamine 6G (R6G), 1,2-bis(4-pyridyl)-ethylene (BPE), tetraethoxysilane (TEOS) (3-mercaptopropyl) trimethoxysilane (3-MPS), 1-octadecanethiol (ODT), isopropanol (IPA), ethanol (EtOH) were obtained from Sigma Aldrich. Sodium hydroxide (NaOH), hydrochloric acid 37% (HCl), sulfuric acid 98% (H_2SO_4), nitric acid 70% (HNO_3), hydrogen peroxide solution 30% in water (H_2O_2), were bought from Carl Roth. All solutions were prepared using Milli-Q water.

The glass slides used as bare substrates were microscope glass slides (Carl Roth, Lauterbourg, France) cleaned with fresh piranha solution (H_2SO_4 (2/3)/ H_2O_2 (1/3)) for 15 min, rinsed with water and dried with nitrogen before use.

All glassware used for gold nanoparticles synthesis was previously washed with freshly prepared aqua regia (HCl (3/4)/HNO₃ (1/4)) followed by extensive rinsing with Milli-Q water.

Klarite[®] 312 surfaces purchased from Renishaw Diagnostics consisted of a square array of gold inverted pyramidal pits made from a (100) silicon wafer etched with KOH solution, and covered with a 300 nm thick evaporated gold layer.

2.2 Solid substrates

2.2.1 Sputtering deposition

Three different substrates were developed by using sputtering deposition with a compact rotary-pumped sputter coater Quorum150RS. The sputtering current intensity has been set at 80 mA for all experiments. Substrate denoted by AuS1 was developed by depositing a nanometric gold film of 25 nm on a glass slide, as described by Degioanni et al. [14] to produce SERS of amorphous silica.

SERS substrate denoted by AuS2 consisted of a gold nanometric film of 25 nm deposited on a glass slide covered by a flat TEOS/3-MPS (1/1) sol film.

The third type of substrate denoted by AuS3 consisted of a square array of gold inverted pyramidal pits microstructure on a glass slide obtained by soft lithography processes [30]. In the first step, a Klarite[®] master template was replicated by replica molding (REM) [30] onto a PDMS mold forming a negative copy of the master. Before the REM of the Klarite[®], an hydrophobic anti-adhesive functionalization was performed using a 2 mM ODT solution in IPA to ensure a successful demolding between Klarite[®] and PDMS. To get the PDMS stamp, mixture of prepolymer and catalyzer (Sylgard 184 elastomer Kit) was poured on Klarite[®] surface and then a curing was performed by heating overnight at 60 °C. PDMS stamp was then carefully removed from the master. In the second step, the PDMS stamp was used to achieve the Klarite[®] positive replica on a glass slide by microtransfer molding (μ TM) of a sol [30]. The sol used for the μ TM consisted of a mixture of TEOS/3-MPS (1/1) and water acidified with HCl. A drop of the sol was deposited onto a glass slide and the PDMS stamp was then deposited by applying a gentle pressure. The residual solvent was removed by evaporation overnight at ambient temperature and the stamp was then removed to obtain the final structure on the glass slide. In a final step, a gold nanometric film of 25 nm was finally deposited on the structure to obtain the active SERS substrate.

All the substrates developed using sputtering deposition are summarized in Table 1.

Table 1 Summary of SERS substrates developed using sputtering deposition

Substrate	Sol	Structure	Gold nanometric film deposited (nm)
AuS1	–	–	25
AuS2	TEOS/3-MPS	–	
AuS3	TEOS/3-MPS	inverted pyramidal pits	

2.2.2 Metallic Nanoparticles Growth on Mesostructured Silica Film

The process begins with electroless growth of silver nanoparticles into mesostructured silica block copolymer films according to the method developed by Bois et al. [31]. Briefly, a sol was prepared by mixing TEOS, F127 block copolymer (PEO)₁₀₆(PPO)₇₀(PEO)₁₀₆, EtOH, water acidified with HNO₃ and AgNO₃. After 1 h of mixing at room temperature, films were deposited by dip-coating and subsequently dried at room temperature for 24 h. The first chemical reduction step can be performed by immersing the film in an aqueous sodium borohydride solution (50 mM) for 30 s. Then, after dipping in water, resultant film showed an intense brownish-yellow coloration due to the formation of first silver seeds in the film. The second step consisted of a total replacement of silver by gold according to Chassagneux et al. [32]. Film previously obtained was immersed during 15 min in 30 mL of water containing 500 μ L of 0.02 M HAuCl₄ and 200 μ L of 0.2 M hydroxylamine solution. The brownish-yellow film coloration gradually disappeared while a pink coloration appeared in the film. The final step consisted of gold seeds growth by immersing the previous film in 30 mL of water containing 500 μ L of 0.02 M HAuCl₄ and 200 μ L of 0.2 M hydroxylamine solution for 15 min leading to active SERS film AuHaS1. AuHaS2 and AuHaS3 films were obtained by repeating this final step one and two times, respectively.

2.3 Gold Nanoparticles Synthesis

2.3.1 Synthesis of Stars-Like Gold Nanoparticles (StAuNPs)

StAuNPs were synthesized by a one-step reduction process described in Minati et al. [28]: a gold precursor is reduced in a basic environment using hydroxylamine as a reducing agent. Briefly, 65 μ L of 0.2 M hydroxylamine aqueous solution were added to 10 mL of 0.01 M NaOH aqueous solution. Then 200 μ L of a 0.02 M solution of HAuCl₄ in water were quickly added under vigorous stirring. The color of the solution changed instantaneously from transparent to deep blue.

2.3.2 Synthesis of Spherical Gold Nanoparticles by Frens Method (FAuNPs)

FAuNPs were synthesized according to Frens method [29]. 50 mL of 0.25 mM HAuCl₄ aqueous solution was heated to boiling and stirred vigorously. Then various amount of 1% sodium citrate aqueous solution was added (1, 0.75, 0.50 or 0.30 mL) and the resultant mixture was kept to boiling and stirred for a further 20 min (30 min for 0.30 mL addition).

2.4 Nanoparticles and Solid Substrates Characterization

Scanning electron microscopy (SEM) pictures were obtained using a Vega 3 (TESCAN). Absorption spectra in the wavelength range of 400–800 nm were measured using UV–vis Agilent 8453 spectrophotometer. Topographic images were obtained with Atomic Force Microscopy (AFM) using an Agilent M5500 instrument operating in tapping mode (Agilent Technologies, Palo Alto, CA, USA). The average resonance frequency of tips was 300 kHz. The root mean square roughness values (RMS) were measured with Gwyddion software on AFM images.

2.5 SERS Measurement

RamanRxn1 spectrometer (Kaiser Optical Systems, Ann Arbor, USA), equipped with a thermoelectrically cooled CCD detector, was used in combination with a sapphire fiber optic immersion probe. Spectra were acquired under 785 nm irradiation (400 mW). For the detection of BPE and R6G, spectra were measured in immersion every 1 min with 5 s data acquisition and 1 spectral accumulation. Data collection was operated using the Holoreact™ software.

2.5.1 Solid Substrates

SERS properties of AuS1 substrates in organic media were studied by measuring BPE and R6G Raman signals after substrates immersion in 5 mL of ethanolic solutions containing between 10⁻¹² and 10⁻³ M BPE or 10⁻⁶ and 10⁻⁴ M R6G. To evaluate SERS effectiveness of AuS1, AuS2, AuS3, AuHaS1, AuHaS2 and AuHaS3 substrates in aqueous media, the substrates were immersed in 5 mL of aqueous solutions containing between 10⁻⁶ and 10⁻⁴ M R6G. SERS spectra were recorded after immersion for 10 min in solution to reach stable signal.

To evaluate the robustness of both the solid substrate manufacturing process and the analysis method, several measurements were achieved: (i) at different locations on a same substrate to evaluate a spot-to-spot reproducibility (ii) using different substrates from the same manufacturing process to investigate a batch to batch reproducibility.

2.5.2 Nanoparticles Suspensions

StAuNPs were firstly tested without the use of any aggregating agent to characterize 10⁻⁶ M R6G aqueous solutions. For this, 50 μL of R6G aqueous solution were added to 5 mL of nanoparticles suspension diluted to a fifth. SERS signal was recorded 30 min after R6G solution addition to reach a stable signal.

StAuNPs were also tested after the addition of HCl as aggregating agent for the characterization of solutions containing from 5.10⁻⁹ M up to 8.10⁻⁸ M of R6G. For this, 50 μL of R6G aqueous solution were added to 5 mL of StAuNPs solution diluted to a fifth to achieve the desired concentration before HCl was added at a concentration of 9.6 mM. SERS signals were recorded 15 min after the addition of HCl to reach a stable signal.

SERS properties of FAuNPs suspensions were studied by characterizing 10⁻⁶ M R6G aqueous solutions with and without the use of NaCl as aggregating agent. For this, 50 μL of R6G aqueous solution were introduced in 5 mL of the colloidal suspension. And then 50 μL of NaCl aqueous solutions were added prior to analysis to reach the final NaCl concentrations reported in Table 2. SERS signals were recorded 10 min after the addition of NaCl or R6G solution to reach a stable signal.

To evaluate SERS signal reproducibility, spectra were acquired for several batches of aggregated nanoparticle suspensions.

2.6 Data Processing

Data analyses were carried out using a spectral window from 1100 to 1700 cm⁻¹ for R6G and from 1500 to 1700 cm⁻¹ for BPE. To reduce baseline drift, spectra were pre-processed by applying a baseline correction using Matlab® R2009b software (Mathworks Inc., Natick MA, USA). For this, Automatic Weighted Least Squares (WLS) algorithm was used [33]: the baseline is estimated by a 2nd order polynomial combined with asymmetric weighting of deviations from the smoothed signal, before to be subtracted from the spectrum.

Table 2 NaCl concentrations used for aggregation of FAuNPs suspensions

Substrate	[NaCl] (mM) tested
FAuNPs 1	0; 5; 10; 20; 40
FAuNPs 2	0; 2,5; 5; 10; 20
FAuNPs 3	0; 0,2; 0,5; 1; 5
FAuNPs 4	0; 0,25; 0,5; 1

3 Results and Discussion

3.1 Raman Characterization of ‘Model’ Analytes

Two molecules commonly used in SERS developments were used as ‘model’ analytes: BPE and R6G, the first being soluble in organic media and the second in organic media and water. The concentration limit of the conventional Raman spectroscopy is between 10^{-3} and 10^{-4} M for both analytes (Fig. 1a, b). BPE characteristic Raman peaks were observed around 1605 and 1645 cm^{-1} and correspond to pyridine ring C=C stretching and the whole ring C=C stretching mode, respectively [15]. R6G characteristic Raman peaks were observed around 1650, 1509 and 1361 cm^{-1} all attributed to the xanthenes ring stretching of C–C vibrations, while the band at 1183 cm^{-1} is related to the C–H bending and N–H bending vibration of xanthenes ring [34].

3.2 In Situ SERS Characterization of Organic Media

The first developed SERS substrate denoted as AuS1 was used for the characterization of BPE in organic media and was made from a glass slide on which a 25 nm gold layer was deposited by sputtering. AFM image of AuS1

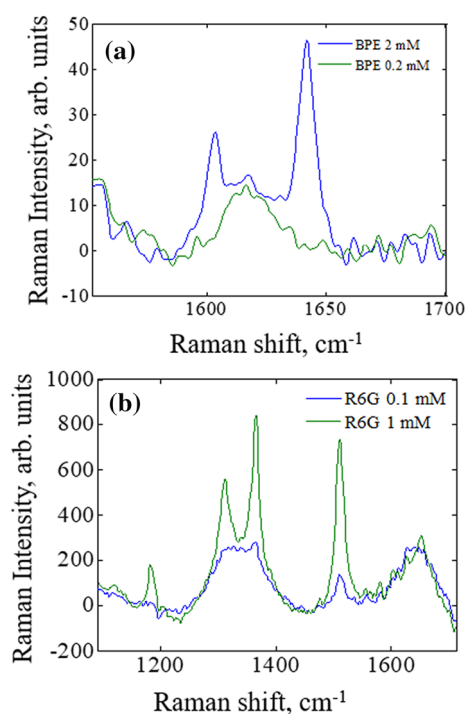


Fig. 1 Raman spectra of 2 and 0.2 mM BPE in ethanol (a) and 1 and 0.1 mM R6G aqueous solutions (b)

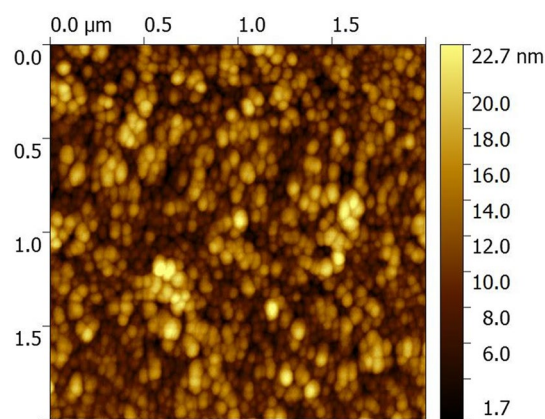


Fig. 2 AFM image of 25 nm thick gold layer sputtered on glass substrate (AuS1)

substrate (Fig. 2) indicated a rough surface made of random assembly of circular particles and characterized by a RMS value of 4 nm.

As shown in Fig. 3a, a significant enhancement of the Raman signal was obtained due to the presence of AuS1 substrate allowing the detection of BPE at very low concentrations down to 10^{-12} M. Results proved the robustness of the developed method with batch-to-batch relative standard deviation (RSD) of about 14% and spot-to-spot RSD of about 12% (Fig. 4). Moreover, as shown in Fig. 3b, a linear relationship characterized by a determination coefficient

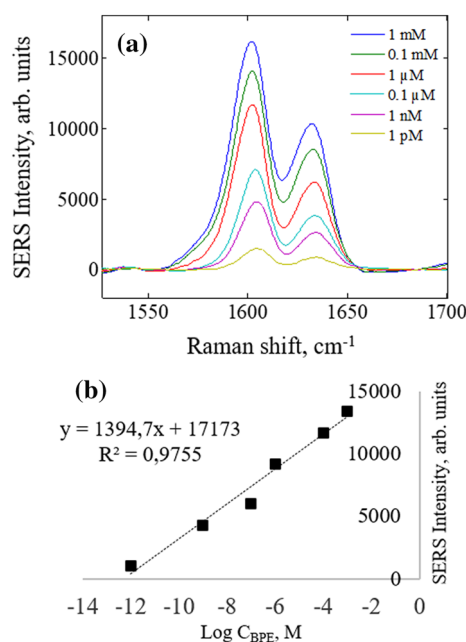


Fig. 3 a Example of SERS spectra obtained from AuS1 SERS substrate as a function of BPE concentration. b SERS signal (1602 cm^{-1}) as a function of BPE concentration for AuS1 SERS substrate in log representation

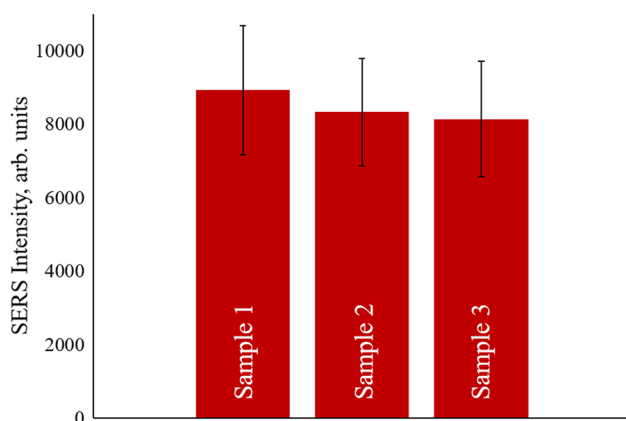


Fig. 4 Study of 10^{-6} M BPE SERS signal reproducibility (at 1602 cm^{-1}) for AuS1 substrate: error bars correspond to spot-to-spot standard deviation determined from measurements at different locations on a same substrate ($n=6$) while the three bars correspond to three different substrates obtained from the same manufacturing process to investigate a batch to batch reproducibility ($n=3$)

$R^2=0.976$ allows to predict from the SERS signal measured at 1602 cm^{-1} the logarithm of BPE concentration (ranging from 10^{-3} to 10^{-12} M). This indicates that the developed method could also be suitable for quantification purpose in organic media.

In the case of the characterization of R6G molecule in the organic media using AuS1 substrate, results appeared less satisfactory since signal became undetectable at concentrations lower than 10^{-6} M (results not shown) even though R6G molecule was more Raman active by using conventional technique (Fig. 1). This difference can't be explained by the electromagnetic mechanism since the same substrate was used for the two molecules. Hence, the difference observed might be due to the involvement of CE which, unlike EE, mainly depends on the interactions between the analyte and the nanostructure. Although CE is commonly considered to be responsible of an increase of the Raman scattering by a factor up to 10–100, observations and theoretical estimates suggest possible contributions from CE as high as 10^5 – 10^7 [35–38]. Another phenomenon which may influence EE and CE, namely the orientation of the adsorbed analyte, could also be involved in the difference observed between BPE and R6G SERS results [39, 40].

3.3 In Situ SERS Characterization of Aqueous Media: SERS Detection and Quantification of R6G

3.3.1 Solid SERS Substrates

3.3.1.1 Sputtering Deposition The analytical method previously developed for the analysis of organic media was first applied to characterize R6G aqueous solutions. But the immersion of AuS1 substrates in this media led to the

quick detachment of the gold deposit making further Raman analysis impossible.

To improve the practical adhesion of the gold deposit at the solid substrate surface, we used a sol film made of TEOS/3-MPS (1/1) deposited on the glass substrate before the gold sputtering deposition. Generally, sol–gel is prepared by the hydrolysis and polycondensation of tetraalkoxysilane. It can be modified with organic functional groups to give so called “ORMOSILs” (for Organically modified silica gels) materials which are inorganic–organic hybrid materials allowing to modify the properties of the resultant sol–gel (i.e. porosity, chemical reactivity, structure, morphology, hydrophobicity...) [41, 42]. Here, thiol groups present in 3-MPS precursor allowed to maintain the integrity of the gold nanometric film thanks to strong gold–thiol interactions.

The use of 3-MPS provided another advantage as a result of the presence of propyl functions in the structure. Indeed, the use of alkyl or aryl derivatives of tetraalkoxysilanes as precursors may provide more flexibility and prevent cracking and shrinking of the coating [43]. Thus, sol film should exhibit suitable rheological features for the replication of structures by soft lithography processes. Here, Klarite® structure has been successfully replicated by using TEOS/3-MPS (1/1) developed sol: the resulting uniform AuS3 substrate consisted of a gold square pyramidal pit pattern of $1.4\text{ }\mu\text{m}$ in width and 900 nm in depth (Fig. 5a, b).

However, no significant evolution of SERS signal from 10^{-4} M R6G aqueous solutions was observed by replacing AuS2 by AuS3 substrate indicating that comparatively a gold-coated pyramidal structure did not lead to significant improvement of SERS signal (Fig. 6). These two substrates provided low variability of the signal measured with spot to spot and batch to batch RSD around 10% (Fig. 6).

3.3.1.2 Metallic Nanoparticles Growth on Mesostructured Silica Film SERS substrates denoted AuHaS1, AuHaS2 and AuHaS3 consisting of gold nanoparticles supported on mesostructured silica film were obtained in a three step procedure. In a first step, silver nanoparticles growth was induced inside the mesostructured silica film by the reduction of silver nitrate contained in the film using sodium borohydride. Then, silver was replaced by gold before finally achieving a growth step of the gold seeds using hydroxylamine as a reducing agent and a gold precursor. As proposed by Chasagneux et al. [32], silver nanoparticles are probably first oxidized by the gold salt giving rise to the formation of hollow and porous gold nanoparticles. These latter are progressively filled with metallic gold consecutively to the Au^{3+} reduction reaction induced by the hydroxylamine agent able to reduce Au^{3+} into preexisting Au^0 [44]. This last feature is then further exploited in the final step of growth of the gold seeds. Figure 7a shows the absorbance spectra obtained

Fig. 5 SEM (a) and AFM (3D) (b) images of AuS3

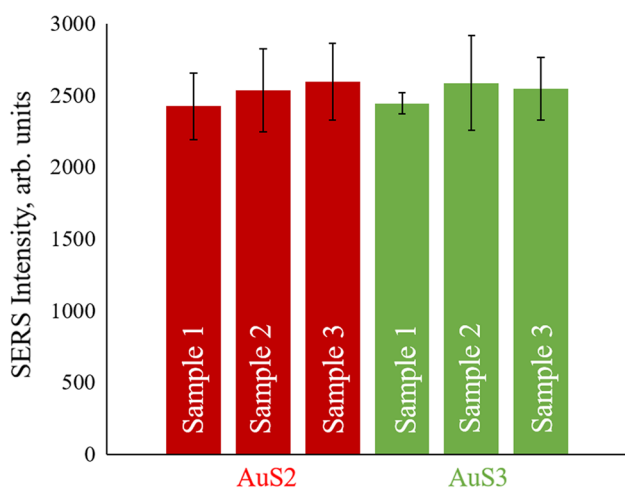
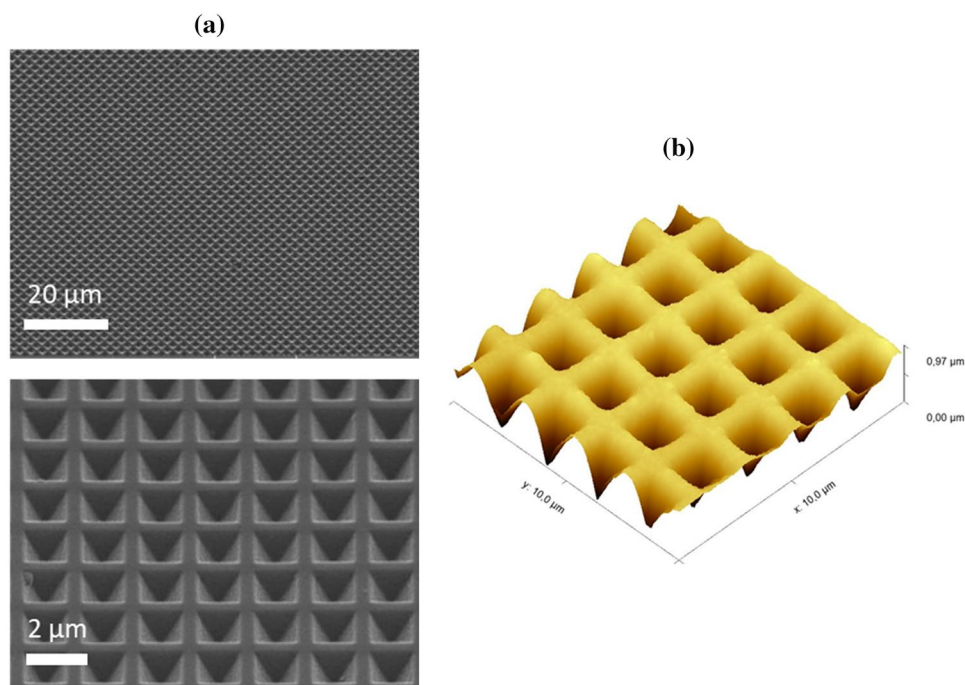


Fig. 6 Study of 10^{-4} M R6G SERS signal reproducibility (at 1362 cm^{-1}) for AuS2 and AuS3 substrates: error bars correspond to spot-to-spot standard deviation determined from measurements at different locations on a same substrate ($n=6$) while the three bars for each type of substrate correspond to three different substrates obtained from the same manufacturing process to investigate a batch to batch reproducibility ($n=3$)

for AuHaS1, AuHaS2 and AuHaS3 substrates. An absorption band centered at about 545–550 nm was observed that may be related to the formation of gold nanoparticles in the film [31, 45]. The slight shift observed for the maximal absorbance characterizing the three substrates can be explained by difference in nanoparticles size. Moreover, the increase of absorbance from AuHaS1 to AuHaS3 should be due to a heightened surface coverage by gold in rela-

tion with the number of growth stage [44]. The increase of both the nanoparticles mean size and the surface roughness (RMS values varied from 42 nm for AuHaS1 to 82 nm for AuHaS3) is observable in AFM images Fig. 7b, c. Figure 8a presents SERS spectra of 10^{-4} M R6G aqueous solutions obtained with AuHaS1 substrate giving similar enhancement of Raman signal than AuS2 and AuS3 substrates with SERS intensities of about 5000 A.U. obtained at 1362 cm^{-1} despite the increasing surface roughness observed. As shown in Fig. 8b, multiplying the number of growth stages led to a loss of spot to spot reproducibility with RSD ($n=6$) of 9% for AuHaS1, 47% for AuHaS2 and 67% for AuHaS3. This higher spot to spot signal variability may be related to a loss of surface homogeneity with the increasing number of unevenly distributed large gold aggregates with the increasing number of growth steps.

3.3.2 Gold Nanoparticles

The enhancement of Raman signal observed with gold solid SERS substrates AuS2, AuS3 and AuHaS1 was very similar and allowed the detection of R6G in aqueous solution with a limit of detection that could be estimated between 10^{-5} and 10^{-6} M. To try to further improve R6G SERS signal, SERS methods using aggregated gold nanoparticles were also developed.

3.3.2.1 FAuNPs Suspensions Several batches of FAuNPs were synthesized by varying the amount of citrate reducing agent to study the influence of the size of nanoparticles on SERS signal (see Table 3). The absorption bands obtained

Fig. 7 **a** Absorbance spectra of AuHaS1, AuHaS2, AuHaS3 substrates and AFM images of AuHaS1 **b** and AuHaS3 **c** substrates

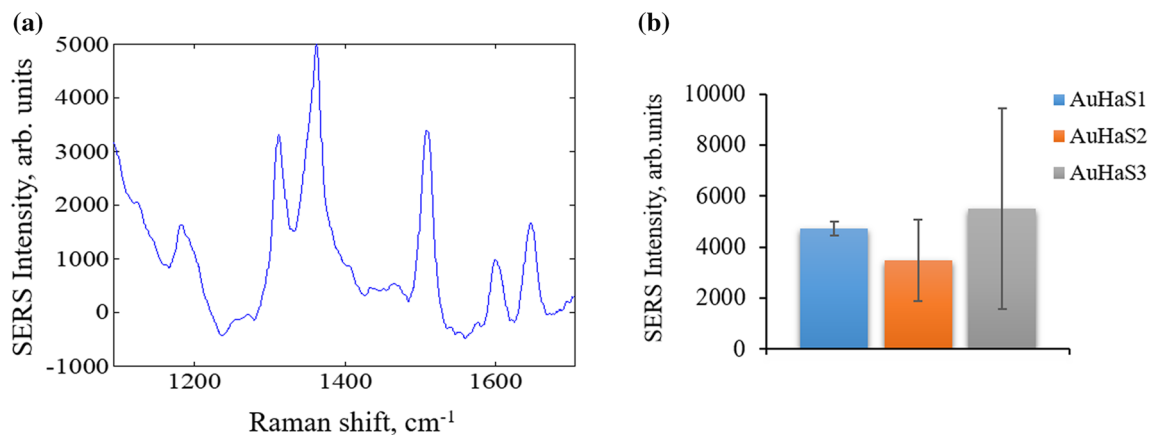
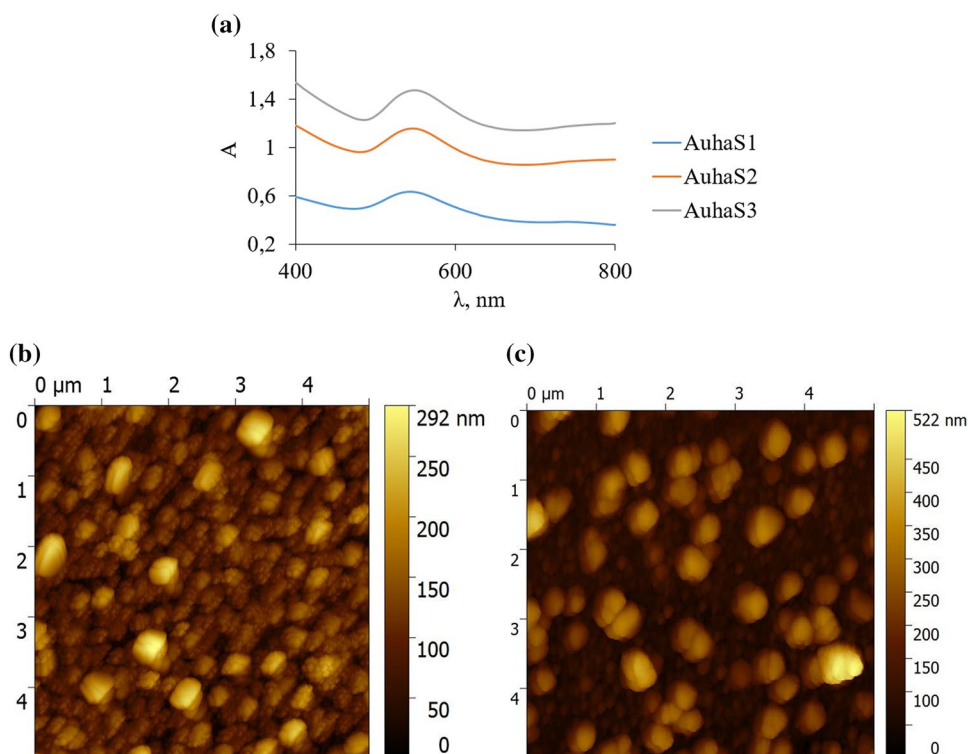


Fig. 8 **a** SERS spectra obtained from 10^{-4} M R6G solution with AuHaS1. **b** Comparison of SERS signal obtained at 1362 cm^{-1} with AuHaS1, AuHaS2 or AuHaS3 SERS substrates in 10^{-4} M R6G aqueous solution (errors bars corresponds to spot-to-spot reproducibility, $n=6$)

Table 3 Mean particle diameters predicted from the wavelength of the maximal absorbance [47] for several batches of FAuNPs

Solution	λ max (nm)	Size (nm)	Quantity of citrate solution 1% (mL)
FAuNPs 1	520	15	1
FAuNPs 2	525	30–40	0.75
FAuNPs 3	530	40–50	0.50
FAuNPs 4	543	70–80	0.30

for FAuNPs suspensions indicated the near-spherical shape of colloid particles with a relatively monodisperse size distribution (results not shown). A broadening of the absorption bands was obtained by decreasing the amount of citrate solution added indicating both an increase of nanoparticles size and polydispersity [46]. The mean particle diameters ranged from 15 to 70 nm (see Table 3)

and was predicted from the wavelength of the maximal absorbance as indicated by Haiss and al. [47].

When nanoparticles are used as SERS substrates, a partial aggregation of the colloids is frequently performed to create “hot-spots” at interparticle junctions. These “hot-spots” are characterized by an extremely high electromagnetic field enhancement necessary for SERS effect [48]. Here, best SERS signals were obtained for FAuNPs 2 and FAuNPs 3 suspensions which exhibited intermediate nanoparticles mean size comprised between 30 and 50 nm (Table 3). In these two cases, a maximum of a twofold increase was observed between SERS signals obtained with and without NaCl. NaCl addition had a more significant impact on the SERS properties of the smallest colloids (FAuNPs 1 of size ~ 15 nm) with a 30-fold increase of SERS signal when NaCl concentration varied from 0 up to 40 mM (Fig. 9). But if a sharp increase of the signal was obtained, SERS intensity remained relatively low (about 10,000 A.U.) and far from the results obtained with the three other formulations (> 50,000 A.U.) (Fig. 9). SERS spectra were acquired for several batches of similar nanoparticles suspensions and here again showing an acceptable reproducibility of the measurements with RSD lower than 15% (Fig. 9).

It should be noted that in the absence of NaCl, the colloid aggregation was induced by the analyte as observed from absorbance spectra (results not shown): an absorbance band

appeared between 700 and 800 nm when adding R6G in FAuNPs 1 suspension due to the localized surface plasmonic resonance (LSPR) feature of aggregated gold nanoparticles while adsorption peak at 520 nm decreased due to the reduction in the number of monomeric gold nanoparticles [49]. Then NaCl addition made the absorbance band between 700 and 800 nm increasingly prominent due to an increasing degree of nanoparticles aggregation [49]. These more aggregated colloids led to significant enhancement of the Raman signal.

3.3.2.2 StAuNPs Suspensions Isolated star-shaped gold nanostructures are supposed to provide a higher amplification of the Raman scattering relative to spherical nanoparticles of the same dimension, since large SERS effect could be obtained at the sharp tips of branches [48, 50]. Moreover, the absence of surfactant in the suspension was of particular interest for proper adsorption of the analyte at nanoparticles surfaces. Indeed, SERS effect takes place only few nanometers at the surface and rapidly decreases with distance [51].

An absorption band centered at about 620 nm was obtained before HCl addition due to the LSPR feature of StAuNPs (results not shown). Then, as observed for FAuNPs, an absorbance band appeared when adding HCl between 700 and 900 nm as evidence of aggregation phenomenon while a decrease of the maximum absorption band

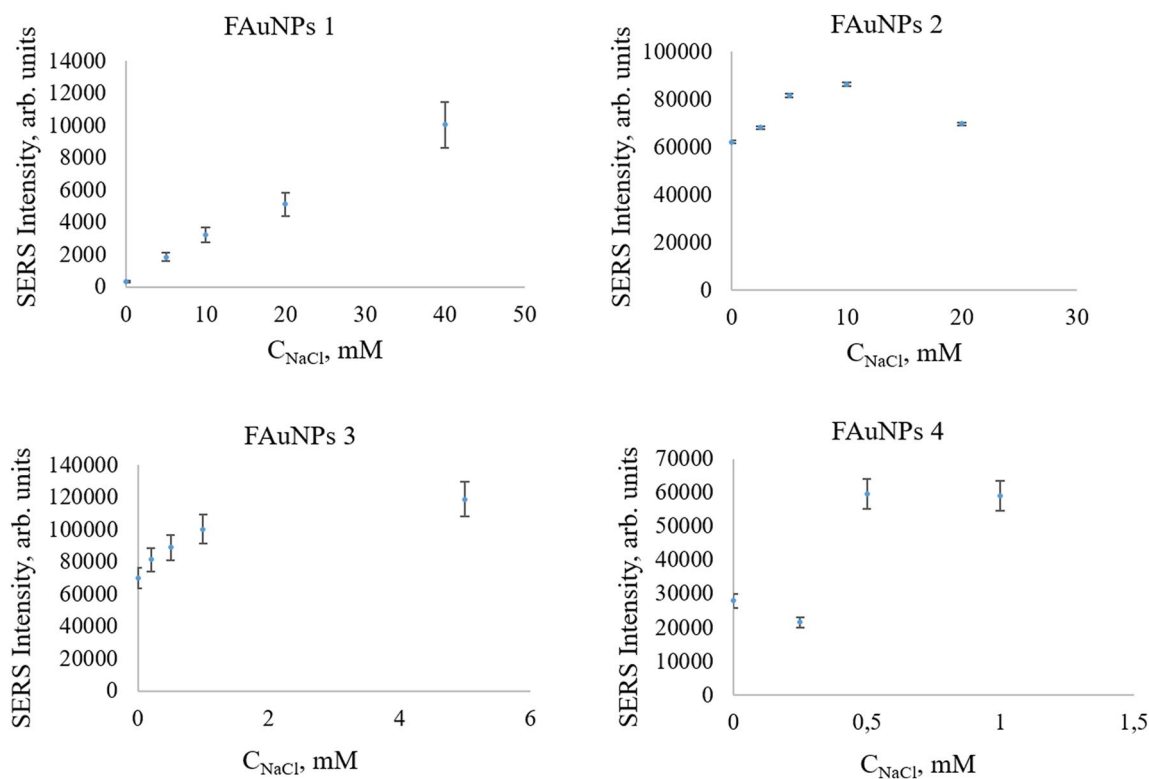


Fig. 9 SERS signal of 10^{-6} M R6G solution obtained with FAuNPs as a function of NaCl concentration (SD, $n=6$)

at shorter wavelength occurred. About 10^3 -fold enhancement of SERS signal was achieved with the use of HCl as aggregating agent.

SERS spectra were acquired for several batches of aggregated nanoparticles in suspension. Results showed a satisfying reproducibility of the measurements with RSD lower than 20%. SERS spectra obtained with StAuNPs after HCl-induced aggregation are presented as a function of R6G

concentration in Fig. 10a. A linear relationship characterized by a determination coefficient $R^2 = 0.984$ allows to predict the R6G concentration (ranging from 8.10^{-8} to 5.10^{-9} M) from the SERS signal measured at 1362.9 cm^{-1} (Fig. 10b). These results show the potential ability of the developed method to quantify analytes in aqueous solutions.

3.4 Comparison of the Developed SERS Substrates

Analytical Enhancement Factor (AEF) was used to roughly estimate and compare the effectiveness of the different substrates developed. AEF can be defined as [52]:

$$AEF = (I_{SERS}/C_{SERS})/(I_{RS}/C_{RS}),$$

where I_{RS} is the Raman signal intensity of an analyte solution at concentration C_{RS} and I_{SERS} is SERS intensity measured with a SERS substrate under identical experimental conditions at concentration C_{SERS} (usually much smaller than C_{RS}) [52]. Using this definition, AEF were determined for each developed substrate and are reported in Table 4.

Enhancement of R6G Raman signal in aqueous media observed with gold solid SERS substrates AuS2, AuS3 and AuHaS1 was very similar with AEF around 5.10^1 (Table 4). These substrates allowed to detect R6G at concentration no much lower than 10^{-5} M. These results appeared quite modest compared to those ($> 5.10^{-6}$ M) observed in the literature for R6G characterization by the means of gold nanostructured solid substrates [53–55]. All the developed gold solid SERS substrates provided relatively reproducible SERS signal with RSD lower than 15%. These reproducibility results are quite in agreement with the literature for SERS solid substrates reporting RSD values between 5 and 20% [9, 10, 18, 19, 53, 56]. As an example, Kalachyova et al. [53] reported MDC of about 10^{-11} M and RSD $< 9\%$ from the analysis at 630 nm of a R6G solution drop deposited onto a SERS surface made of gold multibranching NPs assembled on silver grating surface.

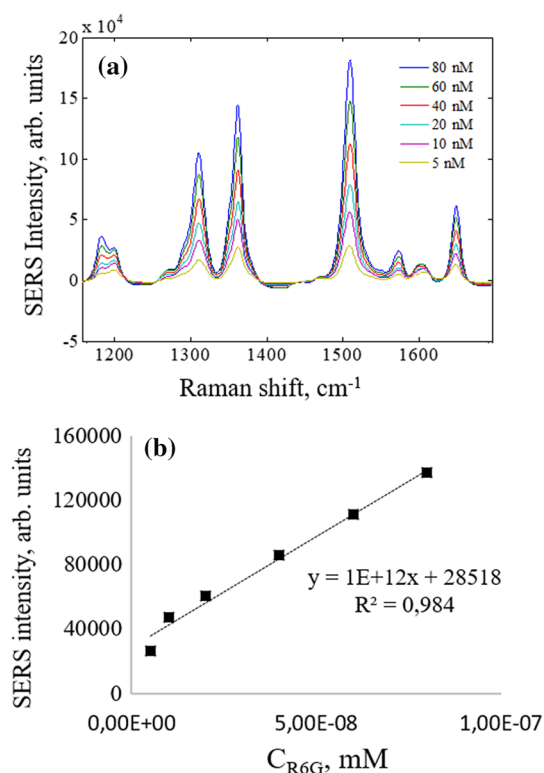


Fig. 10 **a** SERS spectra as a function of R6G concentration for StAuNPs after HCl addition. **b** SERS signal (1362.9 cm^{-1}) as a function of R6G concentration for StAuNPs after HCl addition

Table 4 Gold SERS substrates characteristics in terms of maximal AEF, minimal detectable concentration and batch to batch RSD

SERS substrate	Maximum AEF		MDC (minimal detectable concentration) mol L ⁻¹		Batch to batch RSD (%)
	R6G (1362 cm^{-1})	BPE (1602 cm^{-1})	R6G	BPE	
AuS1	5.10^1 ^b	1.10^{11}	1.10^{-5}	1.10^{-12}	< 15
AuS2	5.10^1 ^a	–	1.10^{-5}	–	< 10
AuS3	6.10^1 ^a	–	1.10^{-5}	–	< 10
AuHaS1	5.10^1 ^a	–	1.10^{-5}	–	–
StAuNPs (after HCl aggregation)	5.10^6 ^a	–	1.10^{-9}	–	< 20
FAuNPs 3 ([NaCl] = 5 mM)	1.10^5 ^a	–	1.10^{-8}	–	< 15

^a in aqueous solution

^b in EtOH solution

By using AuS1 substrate in EtOH solution, AEF remained in the same order of magnitude (~ 5.10) for R6G while reaching very high value ($\sim 1.10^{11}$) for BPE. This demonstrated the high analyte dependence of the SERS enhancement and could be explained by the intervention of CE.

Finally, nanoparticles in suspension clearly provided more effective enhancement of R6G SERS signal than gold solid substrates with a maximum AEF of 5.10^6 obtained with StAuNPs that allowed to detect R6G at concentrations lower than 10^{-9} M. This increase of exaltation efficiency was accompanied by a slight loss of reproducibility with a batch to batch RSD lower than 20% which remained acceptable. It can also be noted that SERS activity of StAuNPs was demonstrated to be higher than that observed with spherical nanoparticles (AEF $\sim 1.10^5$) (see Table 4).

4 Conclusion

In this study, we developed rapid and easy to use SERS methods suitable for the in situ characterization of analytes in aqueous or organic media. For this purpose, different gold substrates (solid surfaces or nanoparticles) were developed to both detect and quantify in situ by SERS two ‘model’ analytes (R6G and BPE). To avoid the use of the SERS mapping technique that is generally encountered with solid substrates to obtain reproducible SERS signal, an unusual probe-based immersion method was successfully used here.

The substrates developed by sputtering deposition of a nanometric gold film on glass slide provided efficient, reproducible and stable BPE SERS signals in organic media making this substrate suitable for quantification purpose at concentration down to 10^{-12} M. However, the minimal signal detectable for R6G molecule in the same organic media appeared clearly unsatisfactory and could be principally explained by a much smaller contribution of the chemical enhancement than BPE to the total signal enhancement.

The use of such substrate for the detection of R6G in aqueous media was made possible by using Tetraethoxysilane/(3-Mercaptopropyl) Trimethoxysilane sol since the integrity of gold nanometric film was maintained through gold–thiol interactions. This same sol was successfully used for the replication of inverted pyramidal pits structure on glass slide by soft lithography processes, but no significant improvement of SERS signal was observed with this structure.

All methods developed with gold solid substrates in aqueous media were clearly less effective than methods employing gold spherical or stars-like nanoparticles that exhibited by far greater enhancement of Raman signal with comparable reproducibility. After an aggregation step, stars-like nanoparticles exhibited the best Raman signal enhancement and the quantification of R6G in aqueous

solution was effective in a concentration range from 8.10^{-8} down to 5.10^{-9} M. Further experiments will be performed to test this promising SERS method for the characterization of bacteria in order to avoid the use of the tedious and time consuming conventional counting method using plating and culturing since the purpose of rapid identification and quantification of microorganisms has become an essential issue in food and water safety, biodefense, human health care and diagnostics.

Compliance with Ethical Standards

Conflict of interest On behalf of all authors, the corresponding author states that there is no conflict of interest.

References

1. Fleischmann M, Hendra PJ, McQuillan AJ (1974) *Chem Phys Lett* 26:163–166
2. Hong S, Li X (2013) *J Nanomater* 2013:1–9
3. Stiles PL, Dieringer JA, Shah NC, Van Duyne RP (2008) *Annu Rev Anal Chem* 1:601–626
4. Schlücker S (2014) *Angew Chem Int Ed* 53:4756–4795
5. Brown RJC, Milton MJT (2008) *J Raman Spectrosc* 39:1313–1326
6. Brolo AG, Irish DE, Smith BD (1997) *J Mol Struct* 405:29–44
7. Creighton JA, Blatchford CG, Albrecht MG (1979) *J Chem Soc Faraday Trans 2(85)*:1851–1997
8. Tognalli NG, Fainstein A, Vericat C, Vela ME, Salvarezza RC (2006) *J Phys Chem B* 110:354–360
9. Fan M, Brolo AG (2009) *Phys Chem Chem Phys* 11:7381–7389
10. Kahl M, Voges E, Kostrewa S, Viets C, Hill W (1998) *Sensors Actuators B Chem* 51:285–291
11. Haes AJ, Haynes CL, McFarland AD, Schatz GC, Van Duyne RP, Zou S (2005) *MRS Bull* 30:368–375
12. Haynes CLC, Van Duyne RPR (2003) *J Phys Chem B* 107:7426–7433
13. Liu GL, Lee LP (2005) *Appl Phys Lett* 87:1–3
14. Degioanni S, Jurdy AM, Cheap A, Champagnon B, Bessueille F, Coulm J, Bois L, Vouagner D (2015) *J Appl Phys* 118:1–7
15. Chu HV, Liu Y, Huang Y, Zhao Y (2007) *Opt Express* 15:12230–12239
16. Merlen A, Chevallier V, Valmalette JC, Lagugné-Labarthe F, Harté E (2009) *Nanotechnology* 20:920–921
17. Freeman RG, Grabar KC, Allison KJ, Bright RM, Davis JA, Guthrie AP, Hommer MB, Jackson MA, Smith PC, Walter DG, Natan MJ (1995) *Science* 267:1629–1632
18. Park HK, Yoon JK, Kim K (2006) *Langmuir* 22:1626–1629
19. Bao L, Mahurin SM, Haire RG, Dai S (2003) *Anal Chem* 75:6614–6620
20. Volkan M, Stokes DL, Vo-Dinh T (2005) *Sensors Actuators B Chem* 106:660–667
21. Yang L, Yan B, Premasiri WR, Ziegler LD, Negro LD, Reinhard BM (2010) *Adv Funct Mater* 20:2619–2628
22. Zhang Q, Lee YH, Phang IY, Lee CK, Ling XY (2014) *Small* 10:2703–2711
23. Ma B, Li P, Yang L, Liu J (2015) *Talanta* 141:1–7
24. Larmour IA, Faulds K, Graham D (2012) *J Raman Spectrosc* 43:202–206
25. Mamián-López MB, Poppi RJ (2013) *Anal Bioanal Chem* 405:7671–7677

26. Abalde-Cela S, Hermida-Ramón JM, Contreras-Carballada P, De Cola L, Guerrero-Martínez A, Alvarez-Puebla RA, Liz-Marzán LM (2011) *Chem Phys Chem* 12:1529–1535
27. Cao Y, Lv M, Xu H, Svec F, Tan T, Lv Y (2015) *Anal Chim Acta* 896:111–119
28. Minati L, Benetti F, Chiappini A, Speranza G (2014) *Colloids Surfaces A Physicochem Eng Asp* 441:623–628
29. Frens G (1973) *Nat Phys Sci* 241:20–22
30. Xia Y, Whitesides GM (1998) *Annu Rev Mater Sci* 28:153–184
31. Bois L, Chassagneux F, Desroches C, Battie Y, Destouches N, Gilon N, Parola S, Stéphan O (2010) *Langmuir* 26:8729–8736
32. Chassagneux F, Bois L, Simon JP, Desroches C, Brioude A (2011) *J Mater Chem* 21:11947–11955
33. Zeng QC, Zhang E, Dong H, Tellinghuisen J (2008) *J Chromatogr A* 1206:147–152
34. Coluccio ML, Das G, Mecarini F, Gentile F, Pujia A, Bava L, Talerico R, Candeloro P, Liberale C, De Angelis F, Di Fabrizio E (2009) *Microelectron Eng* 86:1085–1088
35. Fromm DP, Sundaramurthy A, Kinkhabwala A, Schuck PJ, Kino GS, Moerne WE (2006) *J. Chem. Phys.* 124:061101
36. Ko H, Singamaneni S, Tsukruk VV (2008) *Small* 4:1576–1599
37. Nikoobakht B, Wang J, El-Sayed MA (2002) *Chem Phys Lett* 366:17–23
38. Zhao LL, Jensen L, Schatz GC (2006) *Nano Lett* 6:1229–1234
39. Grochala W, Kudelski A, Bukowska J (1998) *J Raman Spectrosc* 29:681–685
40. Schneider S, Grau H, Halbig P, Freunsch P, Nickel U (1996) *J Raman Spectrosc* 27:57–68
41. Mackenzie JD (1994) *J Sol Gel Sci Technol* 2:81–86
42. Dean SL, Stapleton JJ, Keating CD (2010) *Langmuir* 26:14861–14870
43. Wang D, Chong SL, Malik A (1997) *Anal Chem* 69:4566–4576
44. Brown KR, Walter DG, Natan MJ (2000) *Chem Mater* 12:306–313
45. Hrapovic S, Liu Y, Enright G, Bensebaa F, Luong JHT (2003) *Langmuir* 19:3958–3965
46. Cyrankiewicz M, Wybranowski T, Kruszewski S (2007) *J Phys Conf Ser* 79:1–6
47. Haiss W, Thanh NTK, Aveyard J, Fernig DG (2007) *Anal Chem* 79:4215–4221
48. Fabris L (2015) *J Opt* 17:1–14
49. Xu JX, Siriwardana K, Zhou Y, Zou S, Zhang D (2018) *Anal Chem* 90:785–793
50. Hao F, Nehl CL, Hafner JH, Nordlander P (2007) *Nano Lett* 7:729–732
51. Mayer KM, Hafner JH (2011) *Chem Rev* 111:3828–3857
52. Le Ru EC, Meyer M, Etchegoin PG, Blackie E (2007) *J Phys Chem C* 111:13794–13803
53. Kalachyova Y, Mares D, Jerabek V, Ulbrich P, Lapcak L, Lyutakov O (2017) *Phys Chem Chem Phys* 19:14761–14769
54. Zhou Q, Meng G, Zheng P, Cushing S, Wu N, Huang Q, Zhu C, Zhang Z, Wang Z (2015) *Sci Rep* 5:1–11
55. Ujihara M, Dang NM, Imae T (2017) *Sensors* 17:1–12
56. Guselnikova O, Postnikov P, Kalachyova Y, Kolska Z (2017) *ChemNanoMat* 3:135–144